J. Fluid Mech. (2003), *vol.* 492, *pp.* 91–100.
DOI: 10.1017/S0022112003005597 Printed in the United Kingdom

Maximum drag reduction in a turbulent channel flow by polymer additives

By TAEGEE MIN[1], HAECHEON CHOI[1,2] AND JUNG YUL YOO[2]

[1]Center for Turbulence and Flow Control Research, Institute of Advanced Machinery and Design, Seoul National University, Seoul 151-744, Korea

[2]School of Mechanical and Aerospace Engineering, Seoul National University, Seoul 151-744, Korea

(Received 19 April 2003 and in revised form 21 June 2003)

Maximum drag reduction (MDR) in a turbulent channel flow by polymer additives is studied using direct numerical simulation. An Oldroyd-B model is adopted to express the polymer stress because MDR is closely related to the elasticity of the polymer solution. The Reynolds number considered is 4000, based on the bulk velocity and the channel height, and the amount of MDR from the present study is 44%, which is in good agreement with Virk's asymptote at this Reynolds number. For 'large drag reduction', the variations of turbulence statistics such as the mean streamwise velocity and r.m.s. velocity fluctuations are quite different from those of 'small drag reduction'. For example, for small drag reduction, the r.m.s. streamwise velocity fluctuations decrease in the sublayer but increase in the buffer and log layers with increasing Weissenberg number, but they decrease in the whole channel for large drag reduction. As the flow approaches the MDR limit, the significant decrease in the production of turbulent kinetic energy is compensated by the increase in energy transfer from the polymer elastic energy to the turbulent kinetic energy. This is why turbulence inside the channel does not disappear but survives in the MDR state.

1. Introduction

Since Toms (1949) reported turbulent drag reduction by polymer additives, there have been many studies on this phenomenon using theoretical, experimental and numerical approaches. The two important findings from experimental studies by Virk *et al.* (1967) and Virk (1971) are the onset of drag reduction and the existence of maximum drag reduction (MDR), indicating that drag reduction does not come from a purely viscous effect of a dilute polymer solution (de Gennes 1990; Sreenivasan & White 2000). The onset of polymer drag reduction means that drag reduction occurs only if the concentration exceeds a threshold value. After the onset, the drag decreases more for larger amount of polymer additives. However, it does not decrease below a certain limit, which is called the MDR asymptote or MDR limit.

In general, MDR is obtained when turbulence disappears and the flow becomes laminar (see, for example, Choi, Moin & Kim 1994; Lee & Choi 2001). However, turbulence survives in the MDR state with polymer additives. Warholic, Massah & Hanratty (1999) experimentally studied MDR by polymer additives. They categorized two different regimes of polymer drag reduction: 'small drag reduction' (SDR) and 'large drag reduction' (LDR). They showed that the two regimes have different trends in the variation of turbulence statistics with increasing polymer concentration. One

of the most noticeable results in their experiments on MDR is that the Reynolds shear stress becomes nearly zero at MDR but turbulence does not disappear. Thus, they concluded that the polymer plays a significant role in sustaining turbulence in the MDR state, because the production of turbulent kinetic energy from the mean flow becomes negligible. Sreenivasan & White (2000) also considered the existence of turbulence in the MDR state to be an important feature, and thus they compared scales of the dissipation of turbulent kinetic energy and the polymer elastic energy. Through the scaling analysis, they suggested that even a small amount of stretching would render the polymer elastic energy comparable to the turbulent kinetic energy.

Min *et al.* (2003) investigated drag reduction by polymer additives in a channel flow using direct numerical simulation. The onset criterion for drag reduction predicted in their study was in excellent agreement with previous theoretical and experimental studies. Transport equations for the kinetic and elastic energy were derived to investigate the effect of the elasticity on drag reduction, using the elastic theory of Tabor & de Gennes (1986). From the energy exchange between the kinetic and elastic energy, they suggested a drag-reduction mechanism as follows. When drag reduction occurs, the turbulent kinetic energy near the wall is absorbed by the polymer and transformed to elastic energy. Then, fluid particles containing the elastic energy stored near the wall are lifted up by the near-wall vortical motion and the elastic energy is released into turbulent kinetic energy or dissipated in the buffer and log layers. Therefore, in order to obtain drag reduction, the relaxation time of the polymer solution should be long enough to transport the near-wall elastic energy to the buffer or log layer. Otherwise, the elastic energy obtained near the wall is released there and an equilibrium state exists in terms of the energy exchange, resulting in no drag change (see Min *et al.* for details).

The objectives of the present study are to compare flow characteristics of the SDR and LDR states, and to propose a mechanism for the MDR asymptote in polymer drag reduction, using direct numerical simulation (DNS) of turbulent channel flow. An Oldroyd-B model (linear Hookean dumbbells) is used to represent the behaviour of the polymer solution. Simulations are conducted for $Re_b = U_b h/\nu = 4000$ based on the bulk velocity U_b and channel height h. The present study complements the work by Min *et al.* (2003), in that they investigate, respectively, the existence of MDR and the onset criterion of drag reduction, both of which are important phenomena found by Virk *et al.* (1967) and Virk (1971). The mechanism of MDR will be elucidated through the energy exchange between the kinetic and elastic energy.

2. Governing equations and numerical method

The non-dimensional governing equations of unsteady incompressible viscoelastic flow with an Oldroyd-B model are as follows:

$$\frac{\partial u_i}{\partial t} + \frac{\partial}{\partial x_j}(u_i u_j) = -\frac{\partial p}{\partial x_i} + \frac{\beta}{Re}\frac{\partial^2 u_i}{\partial x_j \partial x_j} + \frac{1-\beta}{Re}\frac{\partial \tau_{ij}}{\partial x_j}, \tag{2.1}$$

$$\frac{\partial u_i}{\partial x_i} = 0, \tag{2.2}$$

$$\tau_{ij} + We\left(\frac{\partial \tau_{ij}}{\partial t} + u_m \frac{\partial \tau_{ij}}{\partial x_m} - \frac{\partial u_i}{\partial x_m}\tau_{mj} - \frac{\partial u_j}{\partial x_m}\tau_{mi}\right) = \frac{\partial u_i}{\partial x_j} + \frac{\partial u_j}{\partial x_i}, \tag{2.3}$$

where u_i is the velocity, p the pressure, τ_{ij} the polymer stress, $Re(=U\delta/\nu)$ the Reynolds number, $We(=\lambda U/\delta)$ the Weissenberg number, U the centreline velocity of the fully developed laminar flow ($U=\frac{3}{2}U_b$), δ the channel half-height ($\delta=\frac{1}{2}h$), ν the kinematic viscosity, λ the relaxation time, and β the ratio of solvent viscosity contribution to the total viscosity of solution. In the present study, $Re=3000$ ($Re_b=U_bh/\nu=4000$; $Re_\tau=u_{\tau_0}\delta/\nu\simeq 135$), and β is fixed to be 0.9 for a viscoelastic fluid. Here u_{τ_0} is the wall-shear velocity for Newtonian fluid flow ($\beta=1$).

As is shown in § 3.1, the amount of drag reduction is very sensitive to the size of the computational domain. Therefore, after a parametric study, we choose the computational domain to be $14\delta\times 2\delta\times 7\delta$ in the streamwise (x), wall-normal (y) and spanwise (z) directions, respectively, with $128\times 97\times 192$ grids ($\Delta x^+\simeq 15$, $\Delta y^+_{min}\simeq 0.3$, $\Delta z^+\simeq 5$). We impose the periodic boundary condition in the streamwise and spanwise directions, and the no-slip boundary condition at the wall. A fully developed turbulent flow field of a Newtonian fluid ($\beta=1$) is used as initial condition for the simulation of viscoelastic fluid flow. A constant mass flow rate is maintained in a channel during simulation by adjusting the mean pressure gradient ($-\mathrm{d}p/\mathrm{d}x$) at each computational time step, i.e. the bulk Reynolds number (Re_b) is constant during simulation.

The numerical algorithm is based on a semi-implicit, fractional step method: the velocity diffusion and polymer stress derivative terms in (2.1) are advanced with the Crank–Nicolson method, and the velocity convection term in (2.1) and all the terms in (2.3) are advanced with a third-order Runge–Kutta method. A fourth-order compact difference scheme is used for the polymer stress derivative $\partial\tau_{ij}/\partial x_j$ in (2.1), and a modified compact upwind difference scheme (Min, Yoo & Choi 2001) is used for the polymer stress convection term $u_m\partial\tau_{ij}/\partial x_m$ in (2.3). All other terms are discretized using the second-order central difference scheme. For the details of the numerical method, see Min *et al.* (2001, 2003).

3. Results

3.1. *MDR asymptote and mean velocity*

The percentage drag reduction (DR) is defined as

$$DR=\frac{(-\mathrm{d}\overline{p}/\mathrm{d}x)-(-\mathrm{d}\overline{p}/\mathrm{d}x|_0)}{-\mathrm{d}\overline{p}/\mathrm{d}x|_0}\times 100, \tag{3.1}$$

where $-\mathrm{d}\overline{p}/\mathrm{d}x$ and $-\mathrm{d}\overline{p}/\mathrm{d}x|_0$ are the time-averaged mean pressure gradients for viscoelastic fluid flow and Newtonian fluid flow, respectively. Figure 1(a) shows the time traces of the mean pressure gradient required to drive a constant mass flow rate in a channel for different Weissenberg numbers; and figure 1(b) shows the variation of drag reduction with the Weissenberg number, plus the amount of drag reduction at $We=5$ when different computational domain sizes are used for simulation. Note that the small domain size results in a completely different transient behaviour and underpredicts the amount of drag reduction. It is clear from figure 1 that the choice of the computational domain size is critical in accurately predicting the amount of drag reduction in the LDR regime and the domain size of $14\delta\times 2\delta\times 7\delta$ provides a fairly converged result. We did not increase the spanwise domain size beyond 7δ because the spanwise two-point correlations of the velocity fluctuations fell off to zero within the separation distance of 3.5δ (half the domain size), indicating that the computational domain is sufficiently large. It is seen that the drag decreases more for larger Weissenberg number in the SDR regime. However, for LDR ($We\geqslant 5$), the amount of drag reduction becomes saturated and approaches the MDR asymptote

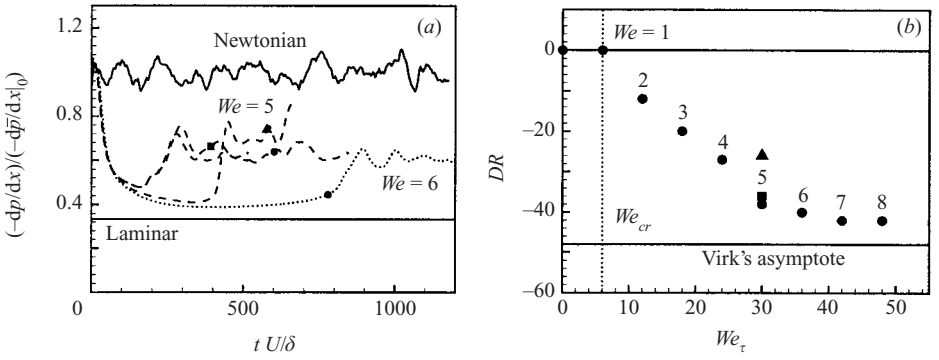

FIGURE 1. (*a*) Time traces of the mean pressure gradient to drive a constant mass flow rate in a channel for different Weissenberg numbers; (*b*) variation of drag reduction with the Weissenberg number. ▲, Computational domain $7\delta \times 2\delta \times 3.5\delta$; ●, $14\delta \times 2\delta \times 7\delta$; ■, $21\delta \times 2\delta \times 7\delta$, respectively. In (*b*), $We_\tau = \lambda u_{\tau_0}^2/\nu$, We_{cr} is the onset Weissenberg number, and the results for $We \leqslant 4$ are from Min *et al.* (2003).

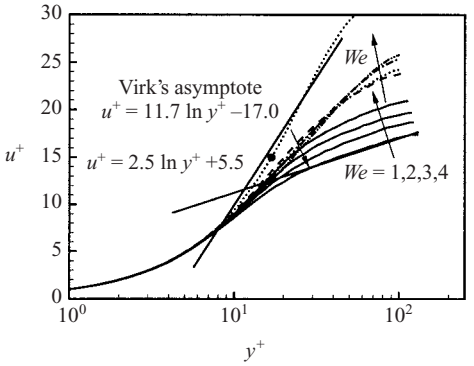

FIGURE 2. Mean streamwise velocities normalized by the actual wall-shear velocity u_τ: ——, Newtonian; – – –, $We = 5$; ·····, $We = 6$; – · – · –, $We = 7$; – ·· – ·· –, $We = 8$. The mean velocity profile obtained during the transient time at $We = 6$ is denoted with ●. Also shown are the mean velocity profiles for $We \leqslant 4$ from Min *et al.* (2003).

of Virk (1971). According to Virk's asymptote, the MDR value increases for higher Reynolds number and it is 48% at $Re_b = 4000$. The amount of MDR from the present study is 44% and this is in good agreement with Virk's asymptote at this Reynolds number, considering that Virk's asymptote was obtained for pipe flow and thus MDR might not be identical to that of channel flow.

It is interesting to note from figure 1(*a*) that, at $We = 6$, the drag decreases substantially in the transient period (up to 60%) and then reaches a fully developed state with less drag reduction (44%). We confirmed the same behaviour for a larger computational domain size of $21\delta \times 2\delta \times 7\delta$. The non-dimensional time to reach the fully developed state after adding polymer additives is about $1000\delta/U$ for $We = 6$, suggesting that a fairly long pipe or channel should be used in experiments to investigate MDR (minimum 400 diameter in length in the streamwise direction when we simply take the convection velocity as the centreline velocity).

The mean velocity profiles normalized by the actual wall-shear velocity u_τ are shown in figure 2. Here, $u^+ = \overline{u}/u_\tau$, $y^+ = yu_\tau/\nu$, and $\overline{u}$ is the mean streamwise velocity. For

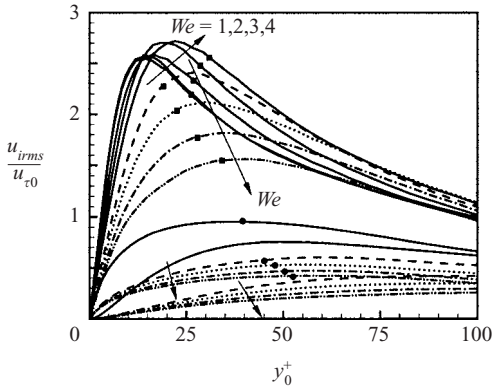

FIGURE 3. Root-mean-square velocity fluctuations normalized by the wall-shear velocity u_{τ_0}. Lines as in figure 2. Lines with ■ denote u_{rms}, plain lines v_{rms}, and lines with ● w_{rms}. Here, $y_0^+ = yu_{\tau_0}/\nu$.

SDR ($We \leqslant 4$), the log-law of the mean streamwise velocity can be expressed as

$$u^+ = 2.5 \ln y^+ + B, \tag{3.2}$$

where $B = 5.5$ for Newtonian fluid flow and B increases for larger drag reduction. However, as seen in figure 2, (3.2) is not valid for LDR ($We \geqslant 5$), and the mean streamwise velocity approaches Virk's asymptotic formula (note that Virk's formula for the mean streamwise velocity was obtained for pipe flow at $Re_b > 10000$). This trend is in good agreement with the experimental results of Warholic *et al.* (1999). However, note that the present mean velocity profile at the MDR state is still quite different from Virk's asymptote. In figure 2, we also plot the mean velocity profile obtained during the transient period at $We = 6$ (see figure 1*a*). Strikingly, this profile nearly falls on Virk's asymptote. Since no asymptotic formula for the mean velocity has been reported in the literature at the low Reynolds number investigated in this study, we do not understand the difference. However, as Virk's asymptotic formula, $u^+ = 11.7 \ln y^+ - 17.0$, was reported for high Reynolds number flows ($Re_b > 10000$) at which maximum drag reduction of more than 60% was obtained, the difference seems to be due to the different amounts of drag reduction at different Reynolds numbers.

In Min *et al.* (2003), DNS were conducted at $Re_b = 4000$ and 20000 in the SDR regime using the Oldroyd-B model, and showed excellent agreement of the simulation data for $Re_b = 20000$ with the previous experimental data. In that study, the simulation at $Re_b = 20000$ was conducted in a minimal channel of sustaining turbulence to reduce the computational cost. In the present study, DNS is performed only at $Re_b = 4000$, mainly because the computational cost for high Reynolds number flow is very high owing to the large computational box size required for LDR. Future large-scale computations at large Reynolds numbers such as $Re_b = 20000$ should be useful.

3.2. *Turbulence statistics*

The root-mean-square (r.m.s.) velocity fluctuations for LDR are shown in figure 3, together with the r.m.s. streamwise velocity fluctuations for SDR from Min *et al.* (2003). All the r.m.s. velocity fluctuations decrease in the whole channel for LDR ($We \geqslant 5$). However, for SDR ($We \leqslant 4$), the r.m.s. streamwise velocity fluctuations decrease in the sublayer but increase in the buffer and log layers. Warholic *et al.* (1999) also reported these trends. The turbulent kinetic energy shows the same trend

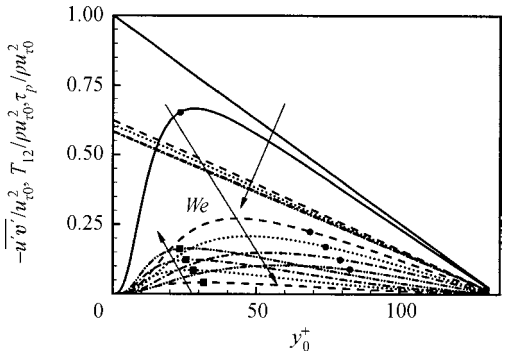

FIGURE 4. Reynolds shear stress, stress deficit and total shear stress normalized by the wall-shear velocity u_{τ_0}. Lines as in figure 2. Lines with ● denote the Reynolds shear stress, lines with ■ the stress deficit, and plain lines the total shear stress.

as the r.m.s. streamwise velocity fluctuations, because u_{rms} is much larger than v_{rms} and w_{rms}. All three components of the vorticity fluctuations substantially decrease with increasing Weissenberg number (not shown here), indicating that the streamwise vortices become weakened and the sweep motion induced by those vortices is less effective in producing high skin friction.

The Reynolds shear stress, $-\rho\overline{u'v'}$, time-averaged stress deficit, τ_p, and total shear stress, $T_{12} = \mu \mathrm{d}\overline{u}/\mathrm{d}y - \rho\overline{u'v'} + \tau_p$, normalized by u_{τ_0} are shown in figure 4. Here, μ and ρ are the viscosity and density of polymer solution, respectively, and τ_p is one of the most interesting features in drag reduction by polymer additives (Gyr & Tsinober 1997; den Toonder *et al.* 1997; Warholic *et al.* 1999). The total shear stress should follow a straight line when the flow reaches a fully developed state, and the present results show that this is indeed the case. The slope of the total shear stress is much smaller than that of Newtonian fluid flow but decreases very slowly with increasing Weissenberg number, because the flow reaches the MDR limit. A significant reduction in the Reynolds shear stress is also observed throughout the channel with polymer additives. For SDR, the slope of the Reynolds shear stress near the channel centre is nearly equal to that of the total shear stress (Min *et al.* 2003), whereas, for LDR, it deviates significantly from that of the total shear stress. The stress deficit τ_p increases remarkably with increasing Weissenberg number and its maximum is in the buffer layer as for SDR (Min *et al.*). However, for SDR, the slope of the stress deficit is negligible around the channel centre, but it is not for LDR, showing a large contribution of τ_p to T_{12} in the LDR regime. This is why the slope of the Reynolds shear stress near the channel centre deviates from that of the total shear stress in the LDR regime. Therefore, the viscoelasticity should be an important property of dilute polymer solutions for drag reduction because the elongational–viscosity hypothesis cannot show the existence of the stress deficit (den Toonder *et al.* 1997). The trend of τ_p in the LDR regime is closely related to the MDR asymptote, which will be discussed in the following section.

3.3. *Polymer elastic energy and the mechanism of MDR*

When the elastic theory of Tabor & de Gennes (1986) is incorporated into the kinetic theory of Bird *et al.* (1987), the time-averaged polymer elastic energy can be expressed

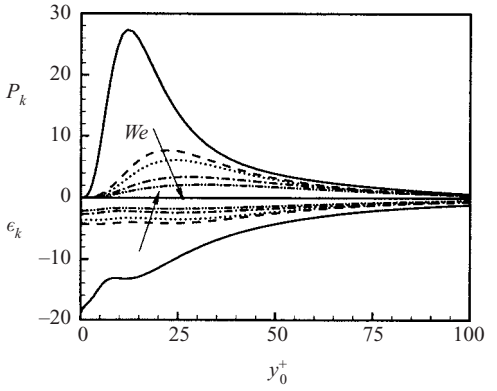

FIGURE 5. Profiles of the production P_k and dissipation ϵ_k of turbulent kinetic energy normalized by $u_{\tau_0}^3/\delta$. The lines as in figure 2.

as (Min *et al.* 2003)

$$k_e = \frac{1}{2}\frac{1-\beta}{Re}\overline{\tau}_{ii}. \tag{3.3}$$

Min *et al.* suggested a drag-reduction mechanism in the SDR regime in terms of the energy transfer between the kinetic and elastic energy. The energy transfer is expressed through the following dynamic equations for the mean kinetic energy (k_m), turbulent kinetic energy (k_t) and polymer elastic energy (k_e):

$$\left\langle \frac{\mathrm{D}k_m}{\mathrm{D}t} \right\rangle = -\langle P_k \rangle - \langle P_{e,m} \rangle + \langle P_w \rangle + \beta \left\langle \frac{1}{Re}\frac{\mathrm{d}^2 k_m}{\mathrm{d}y^2} \right\rangle - \beta \langle \epsilon_m \rangle, \tag{3.4}$$

$$\left\langle \frac{\mathrm{D}k_t}{\mathrm{D}t} \right\rangle = \langle P_k \rangle - \langle P_{e,t} \rangle + \beta \left\langle \frac{1}{Re}\frac{\mathrm{d}^2 k_t}{\mathrm{d}y^2} \right\rangle - \beta \langle \epsilon_k \rangle, \tag{3.5}$$

$$\left\langle \frac{\mathrm{D}k_e}{\mathrm{D}t} \right\rangle = \langle P_{e,m} \rangle + \langle P_{e,t} \rangle - \frac{1}{We}\langle k_e \rangle, \tag{3.6}$$

where

$$k_m = \tfrac{1}{2}\overline{u}^2, \quad k_t = \tfrac{1}{2}\overline{u_i' u_i'}, \quad P_k = -\overline{u'v'}\frac{\mathrm{d}\overline{u}}{\mathrm{d}y}, \quad P_{e,m} = \frac{1-\beta}{Re}\overline{\tau}_{12}\frac{\mathrm{d}\overline{u}}{\mathrm{d}y},$$

$$P_w = -\overline{u}\frac{\mathrm{d}\overline{p}}{\mathrm{d}x}, \quad \epsilon_m = \frac{1}{Re}\frac{\mathrm{d}\overline{u}}{\mathrm{d}y}\frac{\mathrm{d}\overline{u}}{\mathrm{d}y}, \quad P_{e,t} = \frac{1-\beta}{Re}\overline{\frac{\partial u_i'}{\partial x_j}\tau_{ij}'}, \quad \epsilon_k = \frac{1}{Re}\overline{\frac{\partial u_i'}{\partial x_j}\frac{\partial u_i'}{\partial x_j}}.$$

Here $\langle\cdot\rangle = (1/V)\int \cdot \,\mathrm{d}V$ and V is the total volume of the computational domain. For details, see Min *et al.* The energy transfer between k_m and k_t takes place through P_k. The energy transfer between k_m and k_e is through $P_{e,m}$, and that between k_t and k_e is through $P_{e,t}$. The turbulent kinetic energy is dissipated by ϵ_k and the elastic energy is dissipated by its damping term k_e/We (i.e. polymer releases elastic energy by damping).

The spatial distributions of P_k and ϵ_k are shown in figure 5. The production and dissipation of turbulent kinetic energy significantly decrease throughout the channel with polymer additives. This is mainly because the Reynolds shear stress is decreased remarkably for LDR as shown in figure 4. Warholic *et al.* (1999) reported that the significant decrease in the Reynolds shear stress results in zero P_k at the MDR state, which means that the mean flow can no longer transfer its energy to turbulence.

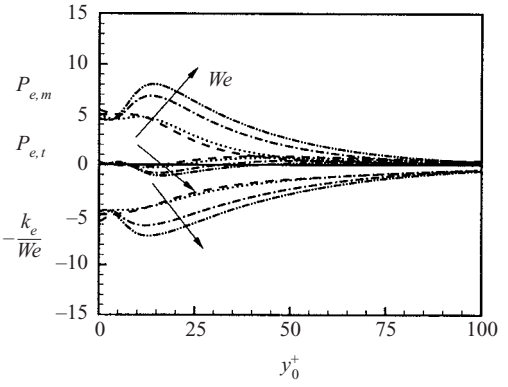

FIGURE 6. Profiles of the productions, $P_{e,m}$ and $P_{e,t}$, and dissipation, $-k_e/We$, of elastic energy normalized by $u_{\tau_0}^3/\delta$. The lines are as in figure 2.

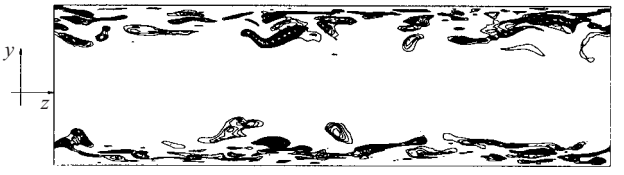

FIGURE 7. Contours of the instantaneous $P_{e,t}$ normalized by $u_{\tau_0}^3/\delta$ for $We = 8$. Here only negative values of $P_{e,t}$ are drawn for clarity and contour levels are from -1 to -30.

Thus, they presumed that turbulence existing in the MDR state originates from the polymer. An interesting observation from figure 5 is that the production is almost zero very near the wall ($y_0^+ < 10$) and the dissipation is nearly constant irrespective of the wall-normal distance, indicating that the near-wall dynamics in a regular turbulent channel flow is clearly destroyed by the polymer in the MDR state.

The spatial distributions of the production and dissipation of elastic energy are shown in figure 6. For SDR, the turbulent kinetic energy near the wall is absorbed by polymer and transformed to elastic energy, and then the elastic energy obtained near the wall is lifted up by the near-wall vortical motion and released into turbulent kinetic energy or dissipated in the buffer and log layers (Min *et al.* 2003). On the other hand, for LDR, the production of turbulent kinetic energy is nearly zero near the wall, so that the same mechanism as for SDR is not expected to be observed. Very near the wall, the production of elastic energy, $P_{e,m}$ (energy transport from the mean flow to the polymer), is balanced by the dissipation, $-k_e/We$, and their magnitudes near the wall in the LDR regime are smaller than those for SDR. Notable is the significant increase in $P_{e,m}$ in the buffer and log layers for LDR, which is mainly caused by the increase in τ_p (figure 4) because $\bar{\tau}_{12} = \tau_p + \mu_E \, \mathrm{d}\bar{u}/\mathrm{d}y$, where $\mu_E = (1-\beta)\mu$. The elastic energy increased from $P_{e,m}$ is either dissipated by damping ($-k_e/We$) or transported to turbulent kinetic energy through $P_{e,t}$. That is, $P_{e,t}$ becomes larger in negative value with increasing We, meaning that the polymer elastic energy returns more energy to turbulence in the buffer and log layers.

Figure 7 shows the contours of negative $P_{e,t}$ inside the channel for $We = 8$ corresponding to LDR. As shown, for $We = 8$ (LDR), energy transfer from the elastic energy to the turbulent kinetic energy ($P_{e,t} < 0$) is very active away from the wall and the magnitude is very large compared to the average value of $P_{e,t}$ at this We (see figure 6 for comparison). Although turbulence decreases more as the flow approaches

the MDR limit, the energy transfer from the elastic energy to turbulence becomes larger simultaneously, which clearly prevents the disappearance of turbulence inside the channel. Therefore, turbulence is sustained even in the MDR state by the transport from the polymer elastic energy to turbulent kinetic energy. With turbulence, the drag at the MDR state is larger than for laminar channel flow, confirming the existence of the MDR limit.

4. Conclusions and further remarks

DNS of turbulent viscoelastic flow in a channel was conducted to investigate the mechanism of MDR by polymer additives. An Oldroyd-B model was used for the polymer stress to represent the viscoelastic nature of polymer solutions. Simulations were carried out by changing the Weissenberg number at the bulk Reynolds number of 4000.

The amount of MDR predicted in the present study was 44%, showing good agreement with Virk's asymptote at this Reynolds number. Experiments showed that the typical log-law for the mean streamwise velocity was not valid for LDR. Instead, the mean streamwise velocity in wall coordinates approached Virk's asymptotic formula, but did not reach it due to the difference in the Reynolds numbers in the present study and Virk's experiments. Furthermore, for LDR, the r.m.s. streamwise velocity fluctuations decreased in the whole channel with increasing Weissenberg number, whereas they decreased in the sublayer but increased in the buffer and log layers for SDR, as also observed in the experimental study.

For LDR, the production of turbulent kinetic energy decreased with increasing Weissenberg number, but the polymer returned more energy from the elastic energy to turbulence simultaneously, preventing the disappearance of turbulence. Therefore, the noticeable effect of polymer additives at the state of MDR was turbulence generation as well as drag reduction.

Finally, we should discuss the validity and limitations of the viscoelastic model adopted in the present study. At present, one of the most feasible macroscopic models for coupled DNS of polymer drag reduction is the two-bead model such as the FENE-P (Sureshkumar, Beris & Handler 1997) and Oldroyd-B models (Min *et al.* 2003). The main reason why we used the Oldroyd-B model is that the elastic energy is easily formulated in an explicit form for linear dumbbells (Oldroyd-B model) but not for nonlinear dumbbells (FENE-P model) (see § 4 in Min *et al.* 2003 for details). Theoretically, however, the polymer stretch in the Oldroyd-B model is not upper bounded, whereas it is bounded in the FENE-P model. Min *et al.* (2003) investigated this issue and showed in the SDR regime that the time evolution of the polymer stretch ($c_{kk}; c_{ij} = We\ \tau_{ij} + \delta_{ij}$) in the Oldroyd-B model is upper bounded due to the finite magnitude of the shear rate in the flow field, and its boundedness is almost the same as that of the FENE-P model. We conducted a separate simulation with the FENE-P model for $We = 6$ to examine the behaviour of the polymer stretch in the LDR regime. As shown in figure 8, the polymer stretch from the Oldroyd-B model does not show any unboundedness and the r.m.s. velocity fluctuations are nearly the same as obtained from the FENE-P model. Therefore, the present results on polymer drag reduction are not model dependent. On the other hand, as Ilg *et al.* (2002) reported in their one-way-coupled DNS (i.e. polymer does not affect the flow), the polymer stretch and orientation of the two-bead macroscopic model may show different behaviours from a multi-bead microscopic model that is believed to be more realistic. Therefore, two-way-coupled DNS with the microscopic model would verify the present MDR mechanism based on the elastic theory.

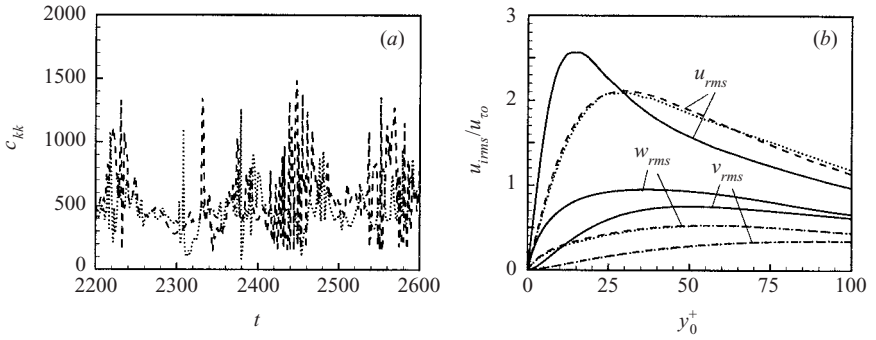

FIGURE 8. (*a*) Time histories of the polymer stretch c_{kk} at $y_0^+ = 10$ and (*b*) r.m.s. velocity fluctuations normalized by $u_{\tau_0}(We = 6)$. ——, Newtonian; – – –, Oldroyd-B model; ·····, FENE-P model with $L^2 = 3600$, where L^2 is the dumbbell extensibility of the FENE-P model.

This study was supported by the CRI of the Korean Ministry of Science and Technology. We are also grateful for useful discussions with Professor Daniel D. Joseph.

REFERENCES

BIRD, R. B., CURTISS, C. F., ARMSTRONG, R. C. & HASSAGER, O. 1987 *Dynamics of Polymeric Liquids, Vol. 2, Kinetic Theory*. John Wiley & Sons.

CHOI, H., MOIN, P. & KIM, J. 1994 Active turbulence control for drag reduction in wall-bounded flows. *J. Fluid Mech.* **262**, 75–110.

DE GENNES, P. G. 1990 *Introduction to Polymer Dynamics*. Cambridge University Press.

GYR, A. & TSINOBER, A. 1997 On the rheological nature of drag reduction phenomena. *J. Non-Newtonian Fluid Mech.* **73**, 153–162.

ILG, P., DE ANGELIS, E., KARLIN, I. V., CASCIOLA, C. M. & SUCCI, S. 2002 Polymer dynamics in wall turbulent flow. *Europhys. Lett.* **58**, 616–622.

LEE, D. & CHOI, H. 2001 MHD turbulent flow in a channel at low magnetic Reynolds number. *J. Fluid Mech.* **439**, 367–394.

MIN, T., YOO, J. Y. & CHOI, H. 2001 Effect of spatial discretization schemes on numerical solutions of viscoelastic fluid flows. *J. Non-Newtonian Fluid Mech.* **100**, 27–47.

MIN, T., YOO, J. Y., CHOI, H. & JOSEPH, D. D. 2003 Drag reduction by polymer additives in a turbulent channel flow. *J. Fluid Mech.* **486**, 213–238.

SREENIVASAN, K. R. & WHITE, C. M. 2000 The onset of drag reduction by dilute polymer additives, and the maximum drag reduction asymptote. *J. Fluid Mech.* **409**, 149–164.

SURESHKUMAR, R., BERIS, A. N. & HANDLER, R. A. 1997 Direct numerical simulation of the turbulent channel flow of a polymer solution. *Phys. Fluids* **9**, 743–755.

TABOR, M. & DE GENNES, P. G. 1986 A cascade theory of drag reduction. *Europhys. Lett.* **2**, 519–522.

TOMS, B. A. 1949 Some observations on the flow of linear polymer solutions through straight tubes at large Reynolds numbers. *Proc. 1st International Congress on Rheology* **2**, 135–141.

DEN TOONDER, J. M. J., HULSEN, M. A., KUIKEN, G. D. C. & NIEUWSTADT, F. T. M. 1997 Drag reduction by polymer additives in a turbulent pipe flow: numerical and laboratory experiments. *J. Fluid Mech.* **337**, 193–231.

VIRK, P. S. 1971 An elastic sublayer model for drag reduction by dilute solutions of linear macromolecules. *J. Fluid Mech.* **45**, 417–440.

VIRK, P. S., MERRIL, E. W., MICKLEY, H. S., SMITH, K. A. & MOLLO-CHRISTENSEN, E. L. 1967 The Toms phenomenon-turbulent pipe flow of dilute polymer solutions. *J. Fluid Mech.* **30**, 305–328.

WARHOLIC, M. D., MASSAH, H. & HANRATTY, T. J. 1999 Influence of drag-reducing polymers on turbulence: effects of Reynolds number, concentration and mixing. *Exps. Fluids* **27**, 461–472.